

# MICROSTRUCTURAL CHARACTERIZATION OF HIGH-PERFORMANCE STEEL FIBER REINFORCED GEOPOLYMER CONCRETE

ZOI G. RALLI<sup>a,\*</sup>, STAVROULA J. PANTAZOPOULOU<sup>a</sup>,  
VLADIMIROG. P. PANGELAKIS<sup>b</sup>

<sup>a</sup> York University, Department of Civil Engineering/Lassonde School of Engineering, 4700 Keele Street,  
Toronto, M3J 1P3, Canada

<sup>b</sup> University of Toronto, Department of Chemical Engineering and Applied Chemistry, 200 College Street  
Toronto, M5S 3E5, Canada

\* corresponding author: zoiralli@yorku.ca

## ABSTRACT.

Due to growing environmental and economic concerns associated with conventional building materials, research interest gravitates towards the development of novel environmentally friendly materials as alternatives to conventional Portland cement concrete. Geopolymer concrete is a class of novel advanced and sustainable structural materials that hold promise for the future of infrastructure. Its synthesis comprises industrial by-products (fly ash and slag among others) in the role of binder and thus reduces the demand in Portland cement leading to a significant carbon footprint reduction. In the present study a High-Performance Fiber Reinforced Geopolymer Concrete (HPFRGC) is synthesized from first principles and is subsequently characterized, with particular emphasis on its microstructural and mineralogical properties. The study explores the linkage between the microstructure and mineralogy of the precursors, and the properties of the final product. Both fresh and hardened HPFRGC are studied. Experimental results illustrate the correlation between microstructure, mineralogy and final mechanical properties can be used as an indicator of suitability of industrial by-products for geopolymer precursors. The effect of these choices on stability and physical properties of the material is also explored in the study.

KEYWORDS: Advanced materials, geopolymer concrete, microstructure, mineralogy, sustainability.

## 1. INTRODUCTION

There is no doubt that nowadays the need for construction building materials has been intensified due to the increase of urbanization rates and the acceleration of global population growth. A commensurate increase in demand for Ordinary Portland Cement (OPC) conventional concrete is expected since construction is a basic leverage of economic development and cement is the cornerstone of the modern infrastructure. However, despite of its widespread use, conventional concrete is not a sustainable solution as it impacts the environment with a potential of considerably high cost for mitigating its implications. Production of cement, as the main component of OPC concrete, is a high-energy consuming process and a major contributor to global warming. Note that for every 1 ton of produced OPC, an equal amount (i.e., 1 ton) of CO<sub>2</sub> is generated. Additional consumption of energy relating to aggregate production and crushing, contributes to the unsustainable depletion of natural resources. It is expected that the green taxes imposed on cement industry as penalty for not reducing the CO<sub>2</sub> footprint will skyrocket the cement price. Consequently, environmental, and economic concerns emerging from the energy intensive

industry of building materials impose a need for re-consideration of every step in their production; one important mitigating strategy is the utilization of innovative alternative cements that have much smaller, or zero CO<sub>2</sub> footprint. Such materials are geopolymer binders, encompassing a variety of industrial wastes in the role of a binder and filler.

Geopolymers represent the latest advancement in alumino-silicate chemistry and they were first developed by Davidovits in the 1970s [1]. Alternative binders are used for their production with activation mechanism, chemistry, and composition fundamentally different from that of cementitious materials. The term Geopolymers refers to mineral compounds, or blends thereof, consisting of repeated units, such as silico-oxide (-Si-O-Si-O-) and silico-aluminate (-Si-O-Al-O-) units, generated through a bonding process called geopolymerization. In this process, many small atomic structures, also known as oligomers, are linked together to form a covalently bonded three-dimensional network. These geo-chemical syntheses occur in the presence of a reactive aluminosilicate material, also known as precursor, either in alkaline medium in the presence of alkali ions such as Na<sup>+</sup>, K<sup>+</sup>, Li<sup>+</sup>, Ca<sup>++</sup> and Cs<sup>+</sup>, or in acidic medium in the

Length $L_f$	Diameter $d_f$	Aspect Ratio $L_f/d_f$	Density $\rho_f$	Tens. Strength $f_t$	Elastic Modulus $E_f$
13 mm	0.2 mm	81.25	7.9 (g/cm <sup>3</sup> )	2500 MPa	200 GPa

TABLE 1. Properties of Steel Fibres.

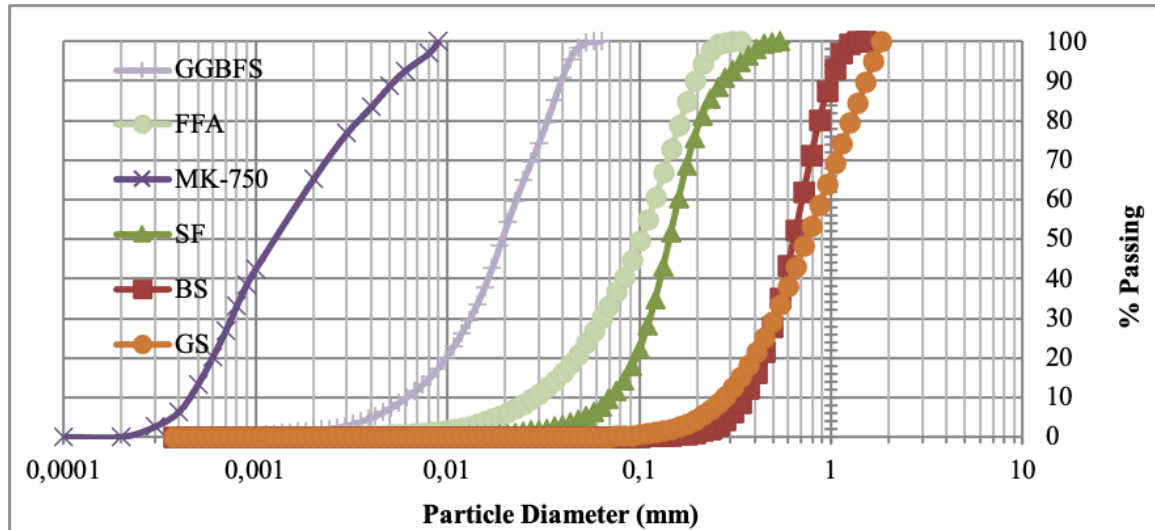


FIGURE 1. Particle Size Analysis of dry materials.

presence of phosphoric and humic acids. Due to the high cost of the latter method, the most common route for geopolymer concrete is the alkaline route especially in the presence of sodium or potassium silicate solutions, which are also known as hardeners [2].

Generally, geopolymer binders demonstrate superior performance and have great advantages over conventional concrete. The development of strength and is not based on a hydration mechanism, but rather on a rigid three-dimensional network formation and is rapid compared to conventional concrete. Contrary to conventional concrete, geopolymer concrete does not possess hydrates in its microstructure; this leads to a higher stability at elevated temperatures [3]. Regarding sustainability and life cycle cost, its production is associated with considerable reduction of the carbon footprint as a result of the absence of cement. In addition, the utilization of industrial waste by-products such as fly ash, blast furnace slag or red mud as source materials provides an additional benefit. It adds value to wastes, while the use of such materials instead of disposal is beneficial for the environment.

The most critical aspect of developing a geopolymer concrete is the right selection of the aluminosilicate source materials. The selection criteria such as high performance and sustainability are determined through deeper understanding of the physico-chemical properties of the material. A suitable source material (i.e., precursor) should be highly amorphous, possess the ability to release aluminium easily and contain sufficient reactive glassy content with low wa-

ter demand. Several studies have been conducted on different types of binders and how they affect the properties of the geopolymer concrete. In literature, a variety of aluminosilicate raw or processed natural materials, such as metakaolin or industrial by-products such as fly ash, as well as granulated blast furnace slag, have been used alone or in combinations as binders for geopolymer concrete and their mechanical and physical properties along with their microstructure have been studied. Despite the growing interest of the research community on the characterization of geopolymer concrete, there is a limited number of investigations that explore the effect of precursor's properties on the properties of the geopolymer concrete.

In the present study, a combination of the most commonly used supplementary cementitious materials, namely metakaolin, fly ash type with CaO less than 10% (Type F), silica fume and blast furnace slag were used for the production of a geopolymer matrix with enhanced early strength and high performance. Industrially produced potassium silicate solution was used as the alkaline reagent, whereas brass coated steel fibres were used for the main reinforcement. Subsequently, the geopolymer was cured at ambient temperature and was then characterized in terms of fresh, hardened, physical, microstructural, and mineralogical properties. A relation between the latter and the raw materials used was also identified.

% Chem.	FFA	SF	MK-750	GGBFS	% Chem. Compos.	FFA	SF	MK-750	GGBFS
SiO <sub>2</sub>	56.5	94.5	52.51	35.2	K <sub>2</sub> O	0.84	0.59	0.19	0.59
Al <sub>2</sub> O <sub>3</sub>	23.5	0.41	43.3	8.37	TiO <sub>2</sub>	0.63	< 0.01	1.42	0.34
Fe <sub>2</sub> O <sub>3</sub>	3.55	0.16	0.47	0.68	P <sub>2</sub> O <sub>5</sub>	0.09	0.08	0.06	0.02
MgO	1.08	0.3	0.05	10.7	MnO	0.06	0.04	< 0.01	0.27
CaO	9.1	0.49	0.08	38.9	Cr <sub>2</sub> O <sub>3</sub>	0.02	0.02	0.03	0.02
Na <sub>2</sub> O	2.13	0.15	0.35	0.31	V <sub>2</sub> O <sub>5</sub>	0.01	< 0.01	0.03	< 0.01
					LOI	1.89	3.5	2.01	2.01

TABLE 2. Chemical Composition of precursors.

## 2. EXPERIMENTAL

### 2.1. MATERIALS

Fly ash type F (FFA), Ground Granulated Blast Furnace Slag (GGBFS), Silica Fume (SF), Metakaolin-750 (MK-750) were used as geopolymer precursors. Basalt (BS) and granite (GS) were chosen as partially reactive sands due to their enhanced bonding with the binder [4]. A commercially available potassium silicate with Molar Ratio (MR) of 1.7 was selected as the hardener (PS) on account of its high performance and stability. Preliminary studies conducted prior to this project, had shown that an industrially produced hardener with a fixed MR performs better than a laboratory made hardener. The better performance is in terms of fluidity and repeatability, while temperature changes do not affect its properties. Straight steel fibers (F) with length 13 mm and diameter 0.2 mm were utilized for main reinforcement at a 2.5% volume fraction (Table 1). Finally, a polycarboxylate-based high-range water reducing admixture (HRWRA) was used to obtain the desired fluidity.

For the best quality control and understanding of the geopolymer concrete, the physical, chemical, and mineralogical properties of the studied precursors were analysed through a series of characterization techniques.

#### 2.1.1. PARTICLE SIZE ANALYSIS

The particle size analysis was performed on a Laser Diffraction Particle size analyser (Beckman Coulter LS 13 320). For very fine particulate materials, surfactants were used for deagglomeration. Figure 1 shows the particle size distribution of the analysed materials.

#### 2.1.2. CHEMICAL ANALYSIS

X-ray Fluorescence (XRF) was performed to get the chemical composition of the precursors. The data given in Table 2 confirm that the aluminosilicate source materials could be potential candidates as geopolymer binders as they contain elevated amounts of alumina and silica in combination with the low magnesia [5]. However, the CaO content in the FFA (close to 10%) poses a concern regarding the speed of setting.

#### 2.1.3. MINERALOGICAL ANALYSIS

The mineralogy of the aluminosilicate source materials is also significant in geopolymerization. For this reason, measurements were made to determine through X-Ray Diffraction (XRD) the mineralogy and degree of crystallinity of the raw materials. Table 3 illustrates the results of the analysis. The presence of mullite and quartz in FFA in combination with the relatively lower amorphous content (compared to the rest) suggests that the combustion temperature of FFA was higher than 850 °C but lower than 1500 °C [6]. GGBFS was found highly amorphous with the presence of gehlenite to be favourable in terms of geopolymerization. However, previous studies have shown that it cannot be used alone as a geopolymer precursor. During alkalination, gehlenite depolymerizes into hydrates and precipitates alkalis. The resulting product is not a geopolymer, but an alkali activated slag, which despite its high strength, there are problems of stability and durability in case the material comes in contact with water. This is because geopolymerization is incomplete and the alkali cation from the hardener is not chemically bonded to the structure [2].

#### 2.1.4. REACTIVITY INDEX

Another reactivity and suitability index was determined through pH measurements. This measurement determines whether there is a risk of flash setting [5]. The pH of aqueous solutions consisting of 5 g of raw material in 50 mL of distilled water was measured after 5 minutes of preparation. Generally, values lower than 8 do not indicate danger for instant hardening, whereas fast hardening occurs for values between 8 and 11 and flash-set is highly possible for values above 11 [5]. The recorded values of pH of the materials are listed in Table 4.

## 2.2. METHODS

Using the data from the characterization steps and taking into consideration cost and sustainability factors, three different mixtures of geopolymer concrete were studied with different ratios of GGBFS to total binder (0%, 5% and 10% of the precursors). The mixture design (Table 5) is based on the fundamental concepts for geopolymerization [7].

Mineral	Mineral Formula	FFA	SF	MK-750	GGBFS
Quartz	SiO <sub>2</sub>	11.1	-	1.4	-
Mullite	2Al <sub>2</sub> O <sub>3</sub> · SiO <sub>2</sub>	19.4	-	-	-
Calcite	CaCO <sub>3</sub>	0.5	-	-	-
Silicon Carbide	SiC	-	2.8	-	-
Gehlenite	2CaO · Al <sub>2</sub> O <sub>3</sub> · SiO <sub>2</sub>	-	-	-	3.2
Alite	3CaO · SiO <sub>2</sub>	-	-	-	1.2
Larnite	2CaO · SiO <sub>2</sub>	-	-	-	1.2
Amorphous		69.0	97.2	98.6	95.4

TABLE 3. Mineralogical Composition of precursors in wt. %.

pH value after 5	FFA (aq.)	SF (aq.)	GGBFS (aq.)	MK(aq.)
	11.5	8.1	11.8	7.1

TABLE 4. pH of aluminosilicate materials.

Materials (kg/m <sup>3</sup> ): Mix Design	FFA	SF	MK-750	GGBFS	K-Silicate Solution	H <sub>2</sub> O	Basalt Sand	Granite Sand	HRWRA
GS10	907	145	75	94	355	71	574	203	18
GS5	907	145	80	47	355	71	574	203	18
GS0	907	145	92	-	355	71	574	203	18

Steel Fibres: All mixes contained 160 kg/m<sup>3</sup>

TABLE 5. Mixture Designs.

### 3. RESULTS & DISCUSSION

#### 3.1. FRESH PROPERTIES

Flowability tests were conducted to evaluate the fresh properties of High Performance Fiber Reinforced Geopolymer Concrete (HPFRGC). The test was performed in accordance with ASTM C1856 [8]. The flowability of each mixture was measured immediately after mixing and right before casting. During this measurement, the conical mould of the flow table was filled with a single layer of fresh geopolymer concrete. Then, the mould was lifted and after one minute, the reported flow value was calculated as the average of maximum and minimum diameter of the spread. The flow values were 157, 172 and 181 mm for the mixtures GS10, GS5 and GS0, respectively. The increase in flowability with the decrease of GGBFS even in such small proportions was evident and linked to the fineness and high CaO content of GGBFS.

The final setting time was also measured empirically as the time from the start of casting to the time the geopolymer completely hardens. The final setting times were 15, 22 and 30 min for the mixtures GS10, GS5 and GS0, respectively. The short setting time was attributed to the high pH of the precursors and particularly the high content of CaO in both GGBFS and FFA.

#### 3.2. COMPRESSIVE STRENGTH

A force-controlled compression-testing machine was used to test the 50 mm cubes under compression at a loading rate of 0.259 MPa/s in accordance with ASTM C39 [9]. To study the age effect on compressive results, the specimens were tested at the age of 1, 7 and 28 days. The compressive strength results of each mixture at different age is presented in Figure 2. Note that the reduction in the GGBFS did not affect the strength at early ages owing to the substitution by MK-750. However, the absence of GGBFS had a more prominent effect on the final strength of GS0.

For the mixing of geopolymer concrete, a 5 L Hobart mixer was used. The mixing process comprises of dry mixing of FFA with SF for 3 minutes, followed by the addition of the alkaline reagent which was mixed with water and high-speed mixing (200 rpm) for 10 minutes. Next, MK-750 is added and mixed for 5 minutes. The last binder material added was GGBFS and was mixed for another 3 minutes. Subsequently the sand mixture was added to the system and the mixing continued for 2 min. At this point HRWRA was introduced to lower the viscosity and prepare the mix for fibre impregnation. When the mix gained the desired fluidity, fibres were added and mixing continued for 2 more minutes. The concrete was then casted in cubic moulds of 50 mm size (minimum dimension had to be about 4-5 times the fibre length). Mild vibration was then performed through the use of tamping rods. Finally, the specimens were

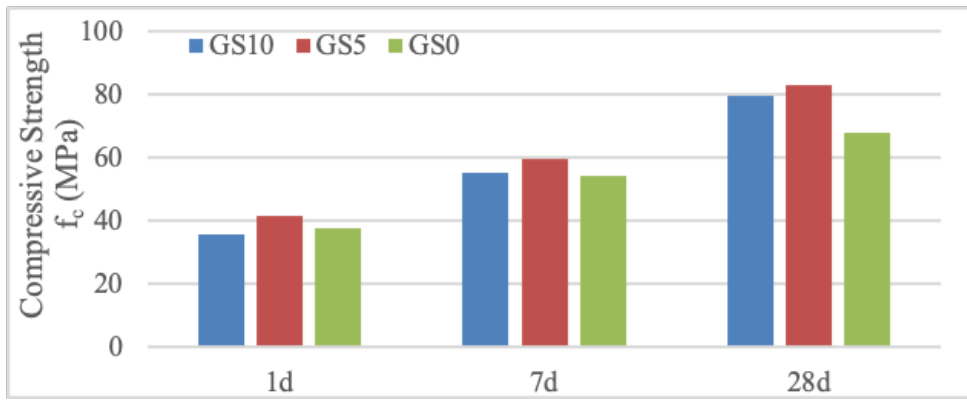


FIGURE 2. Compressive strength development of HPFRGC.

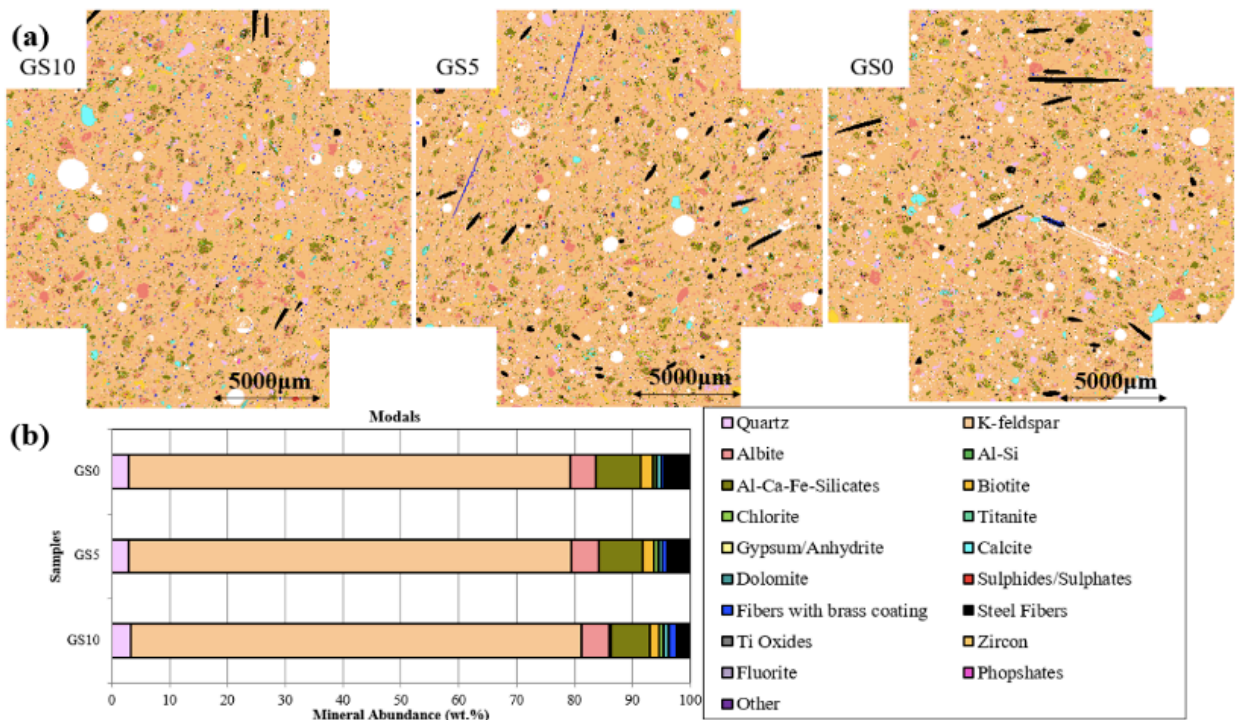


FIGURE 3. QEMSCAN images of HPFRGC thin sections. (a) Phase assemblage maps (b) total mineral contents of each sample by mass.

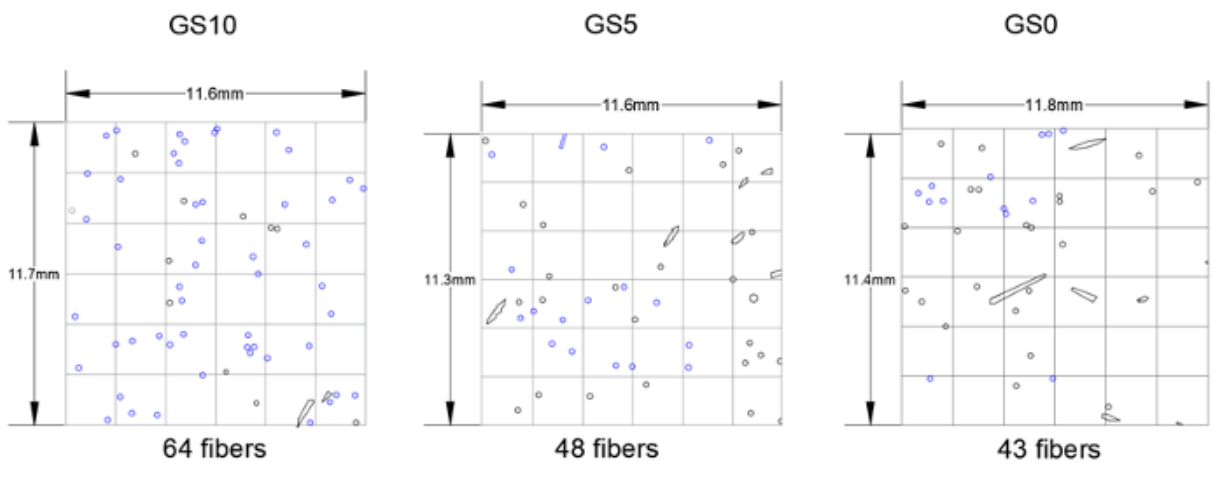


FIGURE 4. Schematic of thin section QEMSCAN images and the number of fibres per cross section.

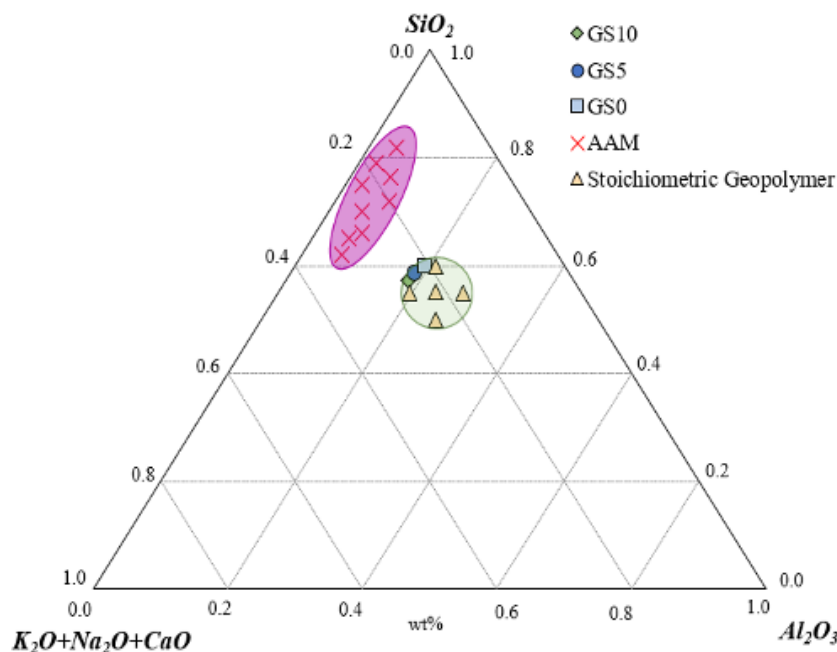


FIGURE 5. Ternary diagram of HPFRGC.

sealed with a plastic sheet to prevent water evaporation. The specimens were demoulded after 24 h and cured in water at ambient temperature until the day of testing.

### 3.3. QEMSCAN ANALYSIS

In order to study the microstructure and mineralogy of the produced geopolymer concrete a QEMSCAN (Quantitative Evaluation of Materials by Scanning Electron Microscopy) analysis was conducted. The system is widely used in the minerals industry as it provides phase and mineral identification at micrometer-scale. Polished thin sections were taken from each HPFRGC cube sample. The QEMSCAN results are illustrated in Figure 3a. The resolution of the produced images is 15  $\mu\text{m}$ . Figure 3b also shows the quantitative composition of the geopolymer mixtures. The mineral maps of all mixtures contain the same major mineral, K-feldspar. The second prevailing mineral is albite. The results agree with what is expected from a geopolymerization process as the K-feldspar and albite are frameworks with 3-dimensional networks. More specifically the produced concrete is a K, Na-Poly(sialate-disiloxo) with atomic ratio Si/Al=3 whereas its geological analogue is sanidine and albite [6]. The white parts of the images represent the porosity. The blue parts correspond to fibres with their brass coating intact while the black represent the steel fibres that have lost their coating during hardening.

### 3.4. FIBER DISTRIBUTION

QEMSCAN images are used as a tool to interpret the distribution of fibres in the thin sections. A schematic

(Figure 4) is used to assess the number of fibres crossing an arbitrary plane, a parameter that is critical for assessing their contribution to the mechanical properties of the solid material. The particles with black and blue colour having a dimension in their short axis at least equal to the fibre diameter  $d_f = 0.2$  mm were identified as fibres (the typical fibre is a cylinder with a diameter of 0.2 mm oriented randomly with respect to the plane of the cross section, therefore in general the intersection has an elliptical shape).

In a random arrangement of fibres, the number of fibres,  $n_f$ , crossing a unit area through HPFRGC is estimated from the cross-sectional area of a single fibre having a diameter ( $d_f$ ) and the volumetric ratio of the fibres,  $V_f$  [10].

$$n_f = 0.64 \frac{V_f}{d_f^2} \quad (1)$$

Equation 1 has been derived assuming only 50% of the fibers to be effective on account of random spatial orientation; for preferential arrangement of the fibers effected by the casting procedure this factor may be higher.

For  $V_f = 2.5\%$  and  $d_f = 0.2$  mm, the  $n_f$  should be 0.4 per  $\text{mm}^2$ . Based on the aforementioned data, ideally the number of fibers at the given randomly cut  $11 \times 11$  mm cross-sections should have been around 54; on average the three samples shown in Figure 5 agree quite well with this estimation.

### 3.5. TERNARY MIX DESIGN

The microstructure of the studied system was assessed by a ternary diagram (Figure 5), plotted from QEMSCAN of the most relevant minerals reported in



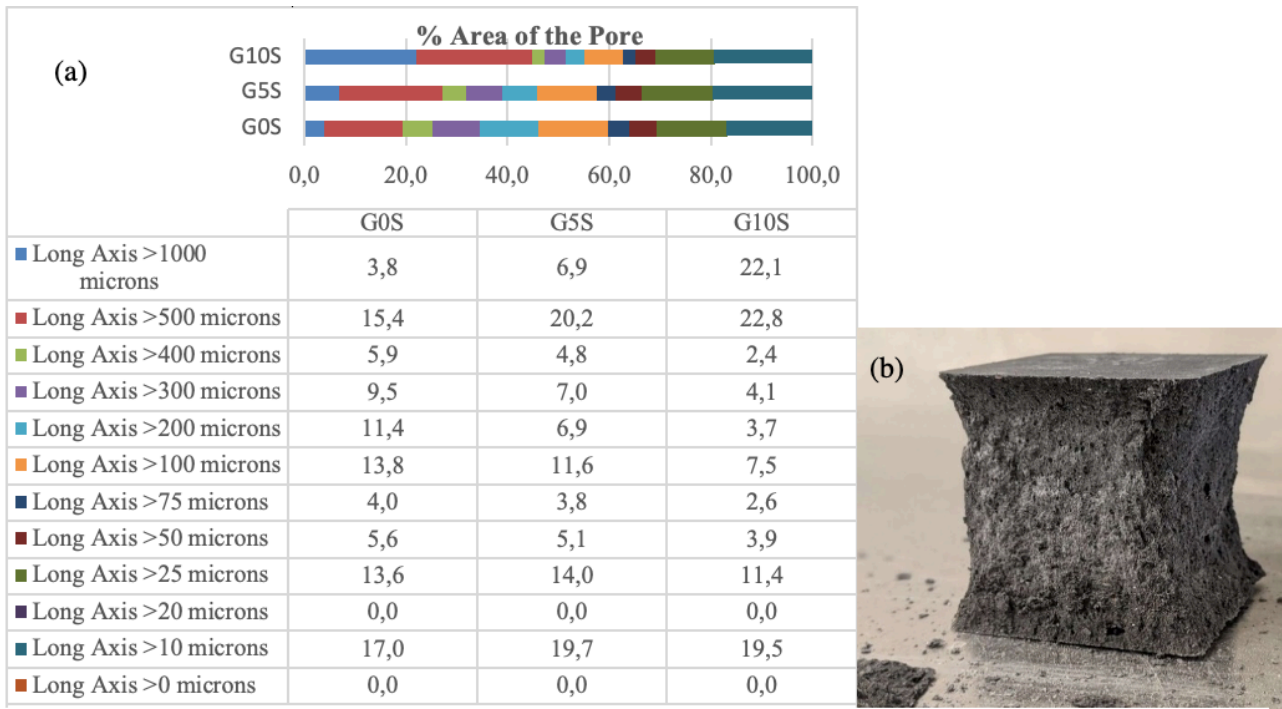


FIGURE 6. (a) Porosity Distribution in HPRGFC measured with QEMSCAN analysis ; (b) Fractured HPGC specimen with bright core at 28 days.

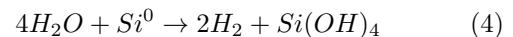
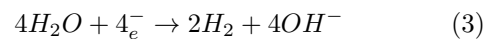
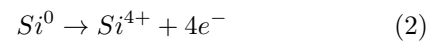
Figure 3b. The corners of the triangle correspond to 100% stoichiometric content of the main oxides, i.e., SiO<sub>2</sub>, Al<sub>2</sub>O<sub>3</sub>, K<sub>2</sub>O, Na<sub>2</sub>O & CaO. The sides represent axes, depicting weight fractions that range from 0 to 1. Any point within the triangle has coordinates on the system of the three axes that represent the fractional ratio of mass content of the standardised oxides; the combination characterizes the stability of physical and durability performance of the resulting composite and therefore may be used to distinguish products that could be classified as alkali activated materials (AAM) from geopolymers. In the present study all the systems show very similar phase assemblage which is relatively close to that of the stoichiometric geopolymer [7].

### 3.6. POROSITY

QEMSCAN images were further used to provide a rough estimation of porosity and its distribution at the analysed thin sections. Figure 6 shows the porosity as a function of size and surface area. The porosity of the HPRGFC can be attributed to three different mechanisms: (a) the production of gas, (b) the fast increase of viscosity with time during casting, and (c) the compaction of the material resulting from simple casting rather than extrusion [11]

The first mechanism is a result of incorporation of SF in the mix design. It is worth noting that studies have shown that even small content (< 1%) of elemental silicon in SF could generate gas approximately 1 to 11 mL/gr of SF [12]. More specifically, this elemental silicon is oxidized in an alkaline environment (Equation 2). H<sub>2</sub> is generated as a result of water

reduction and acts as a foaming agent (Equation 3). The overall reaction forms Si(OH)<sub>4</sub> as shown in Equation 4. The chemically induced porosity seems to yield micropores in the range of 0 – 50 μm. This is clearly shown in Figure 6 where the porosity distribution is depicted demonstrating that all mixtures have similar percentages of 0 – 50 μm micropores.



The increased viscosity due to the addition of very fine and high-density particles such as SF, MK-750 and GGBFS and the incorporation of the fibres also contributes to the pore formation as the diffusion of the generated gas is enhanced [11].

Finally, compaction also affects the porosity, as it depends on the viscosity of the mixture. In case of G10S, the mixture with the highest amount of GGFBS was difficult to compact as much as the other two. This is evident from the high content of pores with maximum size greater than 500 μm in G10S, as shown in Figure 6(a).

Owing to the micropores generated as described above the geopolymer materials are generally lightweight with an apparent density lower than 2 kg/L. For example, the self-weight of the three mixtures tested was 1.9 kg/L. After testing the cubes in compression, and upon examination of fragments from the core of the failed specimens, a whiteish

discoloration was observed. Since this phenomenon could not be studied thoroughly in the HPFRGC broken cubes, as they maintained their integrity on account of the embedded fibres, a series of unreinforced high performance geopolymer concrete cubes were tested in compression to study their fracture surface. Although the specimens were cured in water, the core of the specimen is brighter than the rest because it is dried. This is illustrated in Figure 6(b). The extent of the dried core area is related to the age of testing, as at the early ages is relatively small while it increases with the time. The reaction of geopolymerization starts from the core and expands through the volume of the material. In the white regions of the core the pores have smaller size compared to the dark regions and with the expansion of the white region (development of geopolymerization) the porosity decreases in the specimen. With the progress of geopolymerization the size of pores becomes gradually smaller, whereas water is expelled as hardening propagates.

#### 4. CONCLUSIONS

From the above experimental investigation, the following conclusions are drawn.

1. A full characterization in terms of physical, chemical, and mineral properties is needed to evaluate the suitability of locally available aluminosilicate source materials as geopolymer binders. The determination of the main precursor should be determined taking into consideration the results of the characterization tests.
2. The phase assemblage of the HPFRGC indicates successful geopolymerization similar to natural rocks such as K-feldspar and albite. The produced HPFRGC is K,Na Poly(sialate-disiloxo).
3. Examining the fresh and hardened properties of HPFRGC, it is concluded that FFA with CaO content close to 10% can be used as main precursor in a geopolymer concrete that can harden in ambient temperature and yield high compressive strengths. However, this is accompanied by progressively shorter setting times as GGBFS is added to enhance the final strength. GGBFS has a negative effect in viscosity too, and thus handling of the material. Finally, the studied HPFRGC is an excellent candidate for cases where early strengths are needed, as the geopolymer concrete developed in 24 h after casting almost half strength it would have developed in 28 days.
4. All the three mixtures have acceptable number of fibers as proven by examining randomly cut sections.
5. The porosity of the studied HPFRGC is induced by chemical reactions, viscosity, and consolidation. For the chemically induced porosity, pretreatment of aluminosilicate materials to eliminate the free

silicon is needed, while workability or viscosity modifying admixtures could be used to decrease the porosity generated from high viscosity and poor consolidation.

#### ACKNOWLEDGEMENTS

The authors duly acknowledge the contributions of Dr. Grammatikopoulos and SGS, Canada in carrying out the characterization and microstructural analysis. The support of Wöellner, and Drain Bros. Excavating Ltd. by donating the alkaline reagent and the basalt and granite sands, respectively, is also acknowledged.

#### REFERENCES

- [1] J. Davidovits. Solid Phase Synthesis of a Mineral Blockpolymer by Low Temperature Polycondensation of Alumino-silicate Polymers, 1976.
- [2] Z. G. Ralli, S. J. Pantazopoulou. State of the art on geopolymer concrete. *International Journal of Structural Integrity* **12**(4):511-33, 2020. <https://doi.org/10.1108/ijsi-05-2020-0050>.
- [3]
- [4] A. Reggiani. Types of Automatic Mixing Systems For Geopolymer Mortar/Concrete Production and 3D Printing Geopolymer Camp 9-11 July 2019, Saint Quentin, France, 2019.
- [5] J. Davidovits. Geopolymer Chemistry & Applications, 4th Ed, *Geopolymer Institute*, Saint Quentin, France, 2015.
- [6] J. Davidovits, M.Izquierdo, X.Querol, et al. The European Research Project GEOASH: Geopolymer Cement Based On European Coal Fly Ashes, Technical Paper 22, Geopolymer Institute Library, 2014. <https://www.geopolymer.org/wp-content/uploads/GEOASH.pdf>.
- [7] W. M. Kriven. Geopolymer-based composites, Ceramic and Carbon Matrix Composites, *Comprehensive Composite Materials II*, Elsevier, Oxford, **8**(5): 269-279, 2018. <https://doi.org/10.1016/B978-0-12-803581-8.09995-1>.
- [8] American Society for Testing and Materials. C1856/C1856M: Fabricating and Testing Specimens of Ultra-High-Performance Concrete, 2017.
- [9] American Society for Testing and Materials (ASTM). C39: Standard Test Method for Compressive Strength, 2005.
- [10] N. D. Archontas, S. J. Pantazopoulou. Microstructural Behavior and Mechanics of Nano-Modified Cementitious Materials Adv. Concr. Constr, *Technopress*, **3**(1):15-37, 2015. DOI:<https://doi.org/10.12989/.2015..3.014>.
- [11] E. Prud'homme, P. Michaud, E. Joussein, et al. Silica fume as porogen agent in geo-materials at low temperature. *Journal of the European Ceramic Society* **30**(7):1641-8, 2010. <https://doi.org/10.1016/j.jeurceramsoc.2010.01.014>.



- [12] M.-H.Zhang, V. M. Malhotra, J. Wolsiefer.  
Determination of Free Silicon Content in Silica Fume  
and Its Effect on Volume of Gas Released from  
Mortars Incorporating Silica Fume. *Aci Materials  
Journal* **97**(5), 2000. [https://www.researchgate.net/profile/Min-Hong-Zhang/publication/250613568\\_Determination\\_of\\_free\\_silicon\\_content\\_in\\_silica\\_fume\\_and\\_its\\_effect\\_on\\_volume\\_of\\_gas\\_released\\_from\\_mortars\\_incorporating\\_silica\\_fume/links/5dcff98492851c382f43f4e9/Determination-of-free-silicon-content-in-silica-fume-and-its-effect-on-volume-of-gas-release-d-from-mortars-incorporating-silica-fume.pdf](https://www.researchgate.net/profile/Min-Hong-Zhang/publication/250613568_Determination_of_free_silicon_content_in_silica_fume_and_its_effect_on_volume_of_gas_released_from_mortars_incorporating_silica_fume/links/5dcff98492851c382f43f4e9/Determination-of-free-silicon-content-in-silica-fume-and-its-effect-on-volume-of-gas-release-d-from-mortars-incorporating-silica-fume.pdf).